METHODS FOR ASSESSING THE STRUCTURAL RELIABILITY OF BRITTLE MATERIALS

A symposium
sponsored by
ASTM Committee E-24
on Fracture Testing
San Francisco, Calif., 13 Dec. 1982

ASTM SPECIAL TECHNICAL PUBLICATION 844
Stephen W. Freiman, National Bureau of Standards, and C. Michael Hudson, NASA Langley Research Center, editors

ASTM Publication Code Number (PCN)
04-844000-30

1916 Race Street, Philadelphia, Pa. 19103

Library of Congress Cataloging in Publication Data

Methods for assessing the structural reliability of brittle materials.

(ASTM special technical publication; 844)
"ASTM publication code number (PCN) 04-844000-30."
Includes bibliographies and index.
1. Fracture mechanics—Congresses. 2. Brittleness—Congresses. 3. Ceramic materials—Congresses. I. Freiman, S. W. II. Hudson, C. M. III. ASTM Committee E-24 on Fracture Testing. IV. Series.
TA409.M46 1984 620.1'126 83-73253
ISBN 0-8031-0265-8

Library of Congress Catalog Card Number: 83-73253

Printed in Baltimore, Md. (b)
October 1984

Contents

Introduction

How can we ensure that ceramic components designed for gas turbine engines, human prostheses, optical communication lines, and many other varied applications will survive the in-service stresses imposed on them? This symposium on Methods for Assessing the Structural Reliability of Brittle Materials was organized under the auspices of two subcommittees of ASTM Committee E-24 on Fracture Testing—Subcommittee E24.06 on Fracture Mechanics Applications and Subcommittee E24.07 on Fracture Toughness of Brittle Nonmetallic Materials—for the purpose of providing a forum for discussion of current and proposed procedures for using fracture mechanics data in the design of structures made from essentially brittle materials.

One of the major concerns in the development of new ceramic components is a lack of knowledge regarding the nature of the flaws that can ultimately lead to failure. Many of the papers in this volume address this question, as well as the question of the extent to which data obtained on large cracks in fracture mechanics specimens can be used to predict the behavior of "real" flaws. The use of crack growth rate data in lifetime prediction and proof-test schemes is also emphasized.

The field of structural reliability prediction is a fast-moving one. Even as this book goes to print, the methods of data acquisition and analysis are being further refined. Nevertheless, the editors feel that this volume provides a very useful compilation of papers describing the current state of the science in this field.

Stephen W. Freiman

National Bureau of Standards, Washington, D.C. 20234; symposium chairman and editor.

C. Michael Hudson

NASA Langley Research Center, Hampton, Va. 23665; symposium chairman and editor.

David B. Marshall[1]

Failure from Contact-Induced Surface Flaws

REFERENCE: Marshall, D. B., **"Failure from Contact-Induced Surface Flaws,"** *Methods for Assessing the Structural Reliability of Brittle Materials, ASTM STP 844*, S. W. Freiman and C. M. Hudson, Eds., American Society for Testing and Materials, Philadelphia, 1984, pp. 3-21.

ABSTRACT: The scattering of acoustic waves by surface cracks is used in ceramics as both a method of nondestructive evaluation and a means of investigating the mechanics of failure from surface damage. Initially, experiments combining acoustic scattering, *in situ* optical observations, and fracture surface observations of controlled indentation flaws provide essential insight into the scattering process and the mechanics of failure. With more complex flaw configurations, such as machining damage, acoustic scattering measurements provide a unique method for examining the micromechanics of failure and thereby establishing a basis for strength prediction. The results indicate important differences between indentation flaws and ideal stress-free flaws, both in their response to applied loading and in their acoustic scattering characteristics. The differences are due to the influence of residual stresses associated with indentation flaws. Machining-induced cracks behave similarly to indentation cracks. A basis for failure prediction from acoustic scattering measurements can be established for indentation cracks and machining cracks but not for ideal stress-free flaws.

KEY WORDS: failure, strength, machining, scratching, indentation, residual stress, nondestructive testing, acoustic scattering, fractography, structural reliability, brittle materials

Valuable insight into the mechanism of failure from surface flaws in brittle materials has been provided by studies of idealized model flaw systems produced by indentation (for example, Vickers or Knoop). These studies have demonstrated that residual stresses are generated by any mechanical contact damage involving irreversible deformation. The residual stresses dominate the cracking associated with the contact during both crack formation and subsequent loading of the cracks to failure. Consequently, the strength of a dam-

[1]Research engineer, Structural Ceramics Group, Rockwell International Science Center, Thousand Oaks, Calif. 91360.

aged surface is not related exclusively to the size of the largest crack produced by the damage, as in the conventional view of failure; rather the strength is dictated by the residual stresses, which are determined by the contact parameters (load, geometry) and the elastic/plastic response of the material during the contact event. Detailed fracture mechanics analyses for indentation cracking have been developed and verified experimentally by direct observations of flaw response [*1-5*].

Application of the residual stress concepts derived for isolated indentation flaws to more complex configurations such as machining damage has been demonstrated by observing the scattering of surface acoustic waves from the cracks associated with the damage. In addition to providing a method for identifying the existence of residual stresses and their dominant role in the failure process, the acoustic scattering experiments establish the basis for a method of nondestructive strength prediction.

The main purposes of this paper are to review the current understanding of the mechanisms of failure from contact-induced surface flaws, with particular emphasis on the damage generated by multipoint surface grinding, and to assess the feasibility of nondestructive evaluation using the scattering of acoustic waves. In addition, some new measurements of surface residual stresses associated with machining damage will be presented.

Isolated Cracks

Mechanics of Failure

The importance of residual stresses in the contact-induced cracking of brittle surfaces is readily demonstrated by observing crack evolution during the controlled loading and unloading of well-defined indenters on optically transparent materials. For sharp indenters such as the Vickers or Knoop, the final crack configurations (Fig. 1) are achieved as the indenter is *removed* from the surface [*1,3*], thus establishing that the driving force for crack formation is provided by a residual stress field. Moreover, since the residual field persists after the contact event, it must supplement any applied loading in driving the cracks to failure. The existence of a postindentation crack-opening force has also been demonstrated by observations of subcritical extension of indentation cracks after indenter removal in materials that are susceptible to environmentally assisted slow crack growth [*5,6*].

Determination of the stress intensity factor, K_r, due to the residual field is central to any fracture mechanics analysis involving indentation cracks. The residual field results from the elastic/plastic nature of the deformation beneath the indenter and may be evaluated in terms of an outward-acting pressure at the boundary of the plastic zone [*1,3*]. For approximately axisymmetric indenters, such as the Vickers pyramid, the plastic zone occupies an almost hemispherical volume centered beneath the indentation (Fig. 1, bottom). If

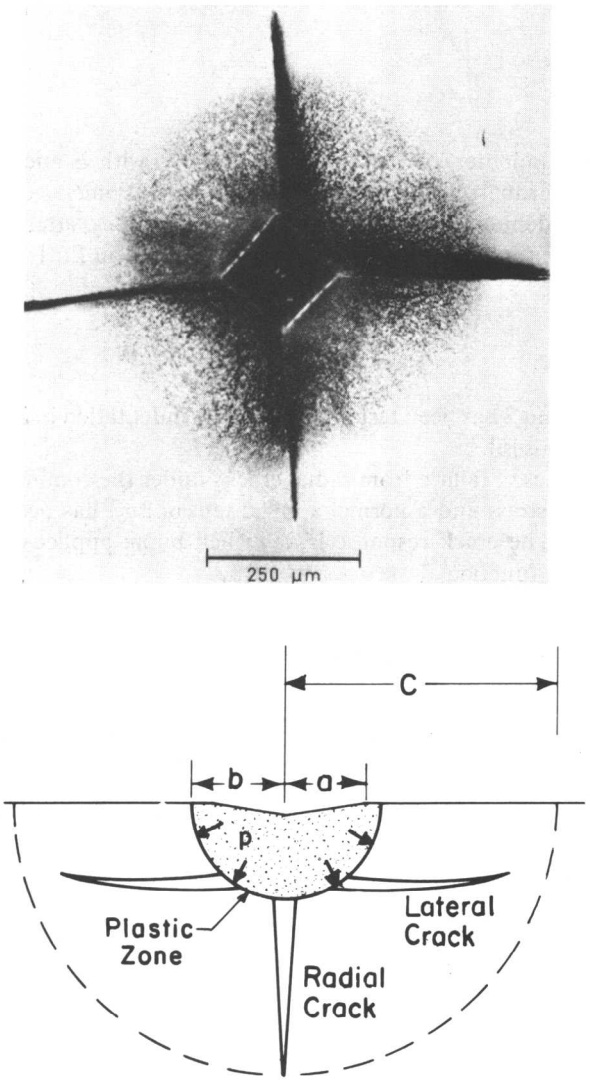

FIG. 1—(Top) *Vickers indentation in zinc sulfide (ZnS).* (Bottom) *Schematic cross section of the indentation, showing the deformation zone and fractures.*

the crack dimension (c) is sufficiently large compared with the plastic zone radius (b) the pressure may be treated as a point force located at the crack center. Under this condition, a straightforward solution for the stress intensity factor for the radial crack has been derived [*1,3*]

$$K_r = \frac{\chi_r P}{c^{3/2}} \tag{1}$$

where P is the indenter load and $\chi_r = \S(E/H)^{1/2}$, with E and H the elastic modulus and hardness of the material and § a dimensionless constant dependent only on indenter geometry. The crack dimension, c_0, after indentation is obtained by equating K_r to the material toughness, K_c, in Eq 1

$$c_0 = \left(\frac{\chi_r P}{K_c}\right)^{2/3} \tag{2}$$

The validity of Eq 2 has been tested with Vickers indentation in a wide range of ceramic materials [5].[2]

The mechanics of failure from radial cracks under the combined influences of the residual stress and a normal applied tension, σ_a, has been analyzed in detail [*2,4,7*]. The crack response is described by an applied-stress/equilibrium-crack-size function

$$\sigma_a = \left[\frac{K_c}{(\pi\Omega c)^{1/2}}\right]\left[1 - \frac{\chi_r P}{K_c c^{3/2}}\right] \tag{3}$$

(where Ω is a crack geometry parameter), which is obtained by superimposing the stress intensity factors due to the residual and applied fields (K_r from Eq 1 and $K_a = \sigma_a(\pi\Omega c)^{1/2}$) and setting $K_r + K_a = K_c$ for equilibrium crack extension. The failure condition is defined by the maximum in the $\sigma_a(c)$ function

$$c_m = \left(\frac{4\chi_r P}{K_c}\right)^{2/3} = 4^{2/3} c_0 \tag{4}$$

$$\sigma_m = \left[\frac{27}{256}\frac{K_c^4}{\chi_r(\pi\Omega)^{3/2}}\right]^{1/3} P^{-1/3} \tag{5a}$$

$$= \frac{3K_c}{4(\pi\Omega c_m)^{1/2}} \tag{5b}$$

[2]This analysis requires that the crack dimensions be large compared with the scale of any microstructure. For example, in large-grained polycrystalline ceramics the fracture resistance becomes dependent on crack length and orientation, resulting in severe disruption of the ideal crack pattern of Fig. 1 [5].

and failure is preceded by stable equilibrium crack growth from c_0 to c_m. This behavior contrasts with the response of ideal, stress-free cracks, where crack instability is achieved at a critical applied stress level without precursor extension ($\chi_r = 0$, $c = c_0$ in Eq 3).

The indentation fracture analysis has also been extended to the linear deformation fracture configuration [*8,9*]. The analysis predicts a similar crack response under applied load, although the region of stable precursor crack growth is more extensive ($c_m/c_0 = 4$) than for axisymmetric penetration ($c_m/c_0 = 2.5$). The linear-damage analysis applies strictly to cracks generated by the penetration of a wedge indenter. However, the observations by Rice and Mecholsky [*10*], of semielliptical (rather than linear) cracks beneath scratches and machining grooves (see also the section on Machining Damage) suggest that loading during machining may resemble more closely axisymmetric indentation. Such geometrical deviations from linear geometry would be expected to reduce the ratio c_m/c_0.

Observations of Crack Response

Optical Observations—In situ measurements of surface traces of indentation cracks during failure testing (Fig. 2*a*) have confirmed the existence of stable precursor crack extension according to Eq 3 in a wide variety of ceramic materials (glass [*2*], silicon [*11*], glass ceramics [*12*], and silicon nitride [*4,13*]). Extensive measurements have been obtained in silicon nitride at various contact loads and indenter geometries [*4,13*]. The data were presented on a universal plot (Fig. 2*b*) by expressing Eq 3 in terms of normalized variables $S = \sigma_a/\sigma_m$ and $C = c/c_m$, so that the parameters describing indenter geometry and contact load do not appear explicitly

$$S = \left(\frac{4}{3}\right)C^{-1/2}\left(1 - \left(\frac{1}{4}\right)C^{-3/2}\right) \tag{6}$$

The crack growth curves for two very different indenter geometries (Vickers and Knoop) are coincident, and both are close to the predicted curve,[3] thus illustrating that Eq 3 applies to a wide range of contact configurations.

Acoustic Scattering Observations—The occurrence of stable crack extension prior to failure from contact-induced flaws provides a convenient indication of the existence of residual crack-opening stresses. For indentation cracks, optical observation of radial surface traces, during load application, has confirmed the expected crack response. However, optical observation of cracks in more general damage configurations such as machining is not always possible.

[3]The increase of crack length with applied stress becomes rapid as σ approaches σ_m. Confirmation that all of the data in Fig. 2*b* represent stable equilibrium cracks was obtained by directly observing the cracks while the applied stress was held constant at each measurement point.

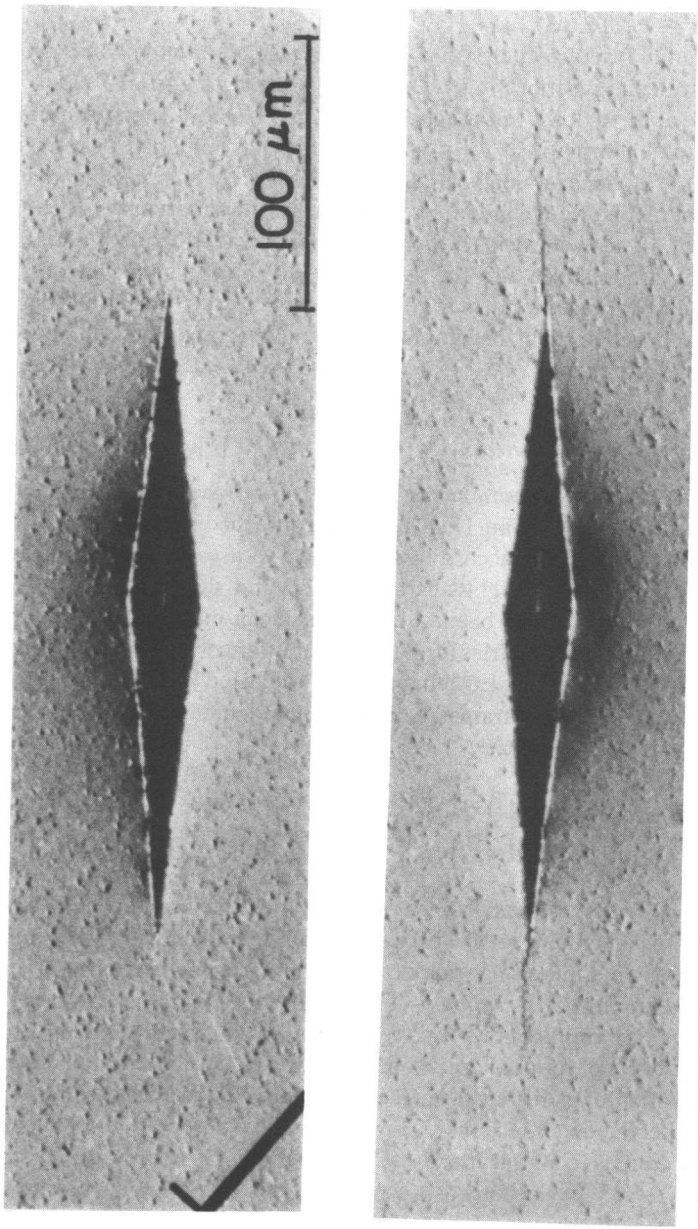

FIG. 2a—*Optical micrographs showing stable crack extension during breaking test: Knoop indentation (50-N load) in* Si_3N_4. *Surface views at the beginning of the breaking test* (top) *and at* $\sigma_a/\sigma_m = 0.9$ (bottom) *(after Ref 4).*

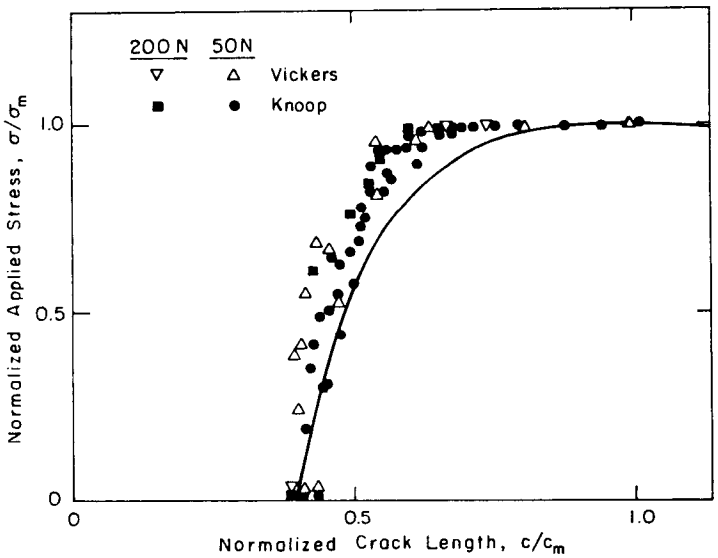

FIG. 2*b*—*Surface trace measurements of stable crack extension during breaking test; Si_3N_4 bars were indented with Vickers or Knoop indenters and broken in bending (after Ref 4).*

In these cases techniques of crack detection based on the scattering of acoustic waves [*14*] provide a means of monitoring crack response and thereby determining the influence of residual stresses.

An acoustic scattering technique designed specifically for the detection of surface cracks [*15*] is illustrated in Fig. 3; transducer 1 excites surface (Rayleigh) waves incident nearly normal to the crack surface, and transducer 2 detects the backscattered waves. The relative amplitude of the backscattered signal is related, by means of scattering analysis, to the crack dimensions, whereas the time delay between the generation and the receiving of the signal defines the crack position.

The acoustic scattering from surface cracks is related uniquely to the crack area, provided the crack surfaces are separated. However, the scattering is sensitive to the existence of crack closure effects. This sensitivity is demonstrated by comparing the acoustic scattering from an indentation crack and an initially stress-free crack[4] of similar dimensions (Fig. 4*a*). Optical observations confirmed that the stress-free crack did not extend prior to failure. However, the reflected acoustic signal (expressed in Fig. 4*a* in terms of a calculated crack radius, assuming an *open*, surface half-penny crack [*16*]) shows a *reversible* increase with applied load. This increase was interpreted in

[4]The stress-free crack was obtained by removing the plastic zone (and therefore the residual stress) of an indentation crack by mechanical polishing. Similar acoustic scattering results have also been obtained from cracks which had the residual stress eliminated by annealing [*15*].

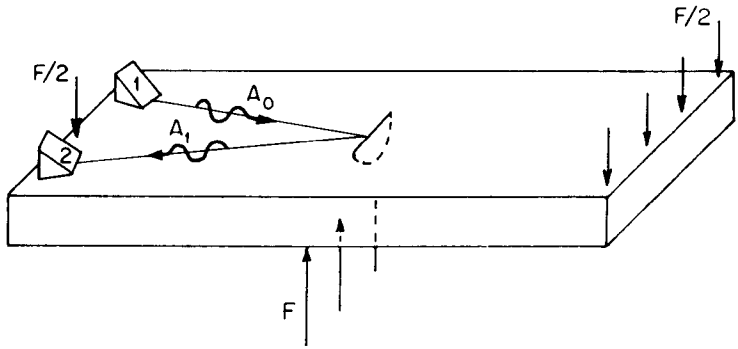

FIG. 3—*The acoustic scattering and mechanical loading configurations used for monitoring crack growth during failure testing:* A_0 = *amplitude of wave excited by transducer 1;* A_1 = *amplitude of scattered wave received by transducer 2;* F = *applied bending force (after Ref 17).*

terms of a reversible opening and closing of the crack surfaces under the applied loading [*15*]. At zero applied stress, complete crack closure is prevented by contacts at asperities over the crack surface. The areas between the contacts scatter as small open cracks of area A_i but, since the scattered amplitude from each open area is approximately proportional to $A_i^{3/2}$ the total scattered amplitude is considerably smaller than that of a fully open crack. Applied tension relieves the contacts continuously until, at the failure point, the crack faces are fully separated and the true crack radius is measured (compare the optical crack length measurement, Fig. 4*a*).

Acoustic scattering from indentation cracks (which are subject to residual crack opening) does not show the reversible opening and closing effects (Fig. 4*b*). However, an *irreversible* increase in acoustic signal with applied tension, corresponding to genuine stable crack extension, is detected. Despite some complication in modeling the crack geometry for acoustic scattering analysis,[5] a true measure of the crack dimension is obtained at all stages during the failure test. Comparison of acoustic measurements, optical measurements, and fracture mechanics predictions (Eq 3) are shown in Fig. 4*c*. The irreversibility of the acoustic scattering response with applied loading provides a definitive indication of the presence of residual crack opening stresses.

The responses of two linear isolated damage configurations (row of indentations, scratch) have also been investigated [*17*]. An irreversible increase in scattered intensity was observed in both cases, thus indicating the existence of stable precursor crack extension due to residual stresses.

[5]The crack does not penetrate the plastic zone; therefore, the crack exhibits the geometry of a semiannulus with inner radius dictated by the plastic zone radius. Calculations based on a subsurface elliptical crack have provided a good approximation [*15*].

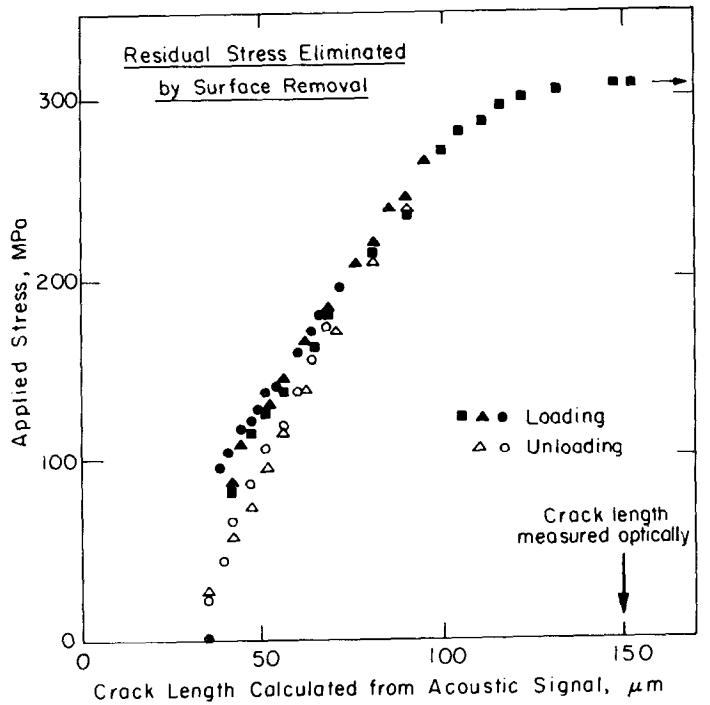

FIG. 4a—*Variation of acoustic scattering, from indentation cracks in polished surfaces of Si_3N_4, during tensile loading: stress-free crack. Note the* reversible *increase in acoustic scattering (expressed as crack length calculated for an open half-penny surface crack) with applied tension.*

Fracture Surface Observations—In some materials the regions of stable and unstable crack extension can be distinguished in optical observations of the fracture surface. The distinction arises from changes in fracture morphology [*17*] (for example, transgranular to intergranular) or from small perturbations in the plane of propagation [*1*]. The fracture surface of a Knoop indentation crack in Si_3N_4 is shown in Fig. 5. The reflectivity (brightness) is high in the regions of crack formation and postfailure extension but low in the intermediate region of stable crack growth during loading.

The fracture surface for a row of Knoop indentation cracks in Si_3N_4 is shown in Fig. 6. Under the influence of the applied tension, some of the cracks coalesced and extended stably to an elongated semielliptical surface crack configuration at failure. Similar crack configurations were observed on fracture surfaces resulting from scratch-induced failures [*17*]. The identification of stable precursor crack growth is consistent with the acoustic scattering results.

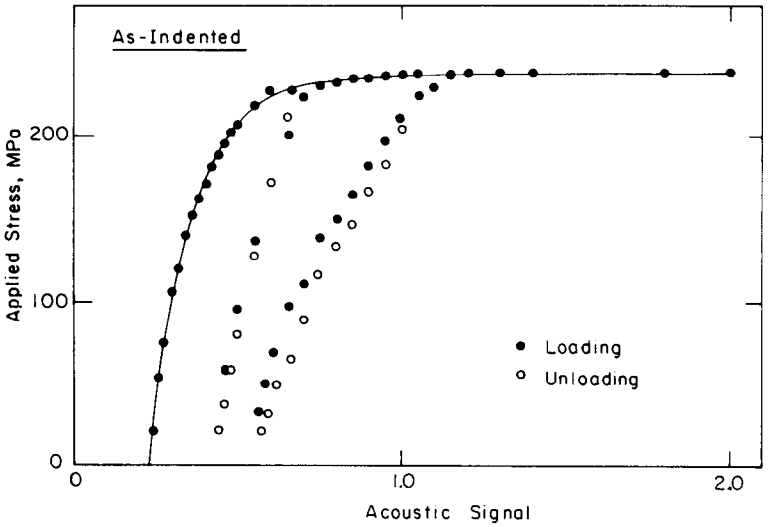

FIG. 4*b*—*Knoop indentation crack (50-N load). Note the* irreversible *increase in acoustic scattering.*

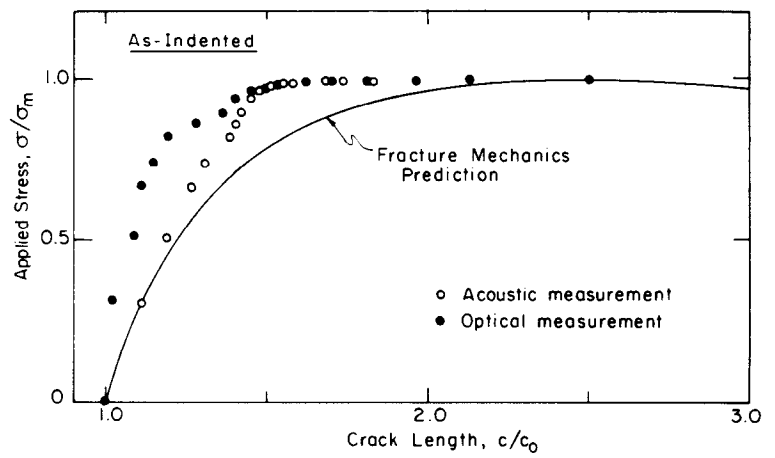

FIG. 4*c*—*Knoop indentation crack (50-N load): comparison of acoustic measurements,* in-situ *optical measurements, and fracture mechanics prediction of the variation of crack length with applied tension (after Ref* 17*).*

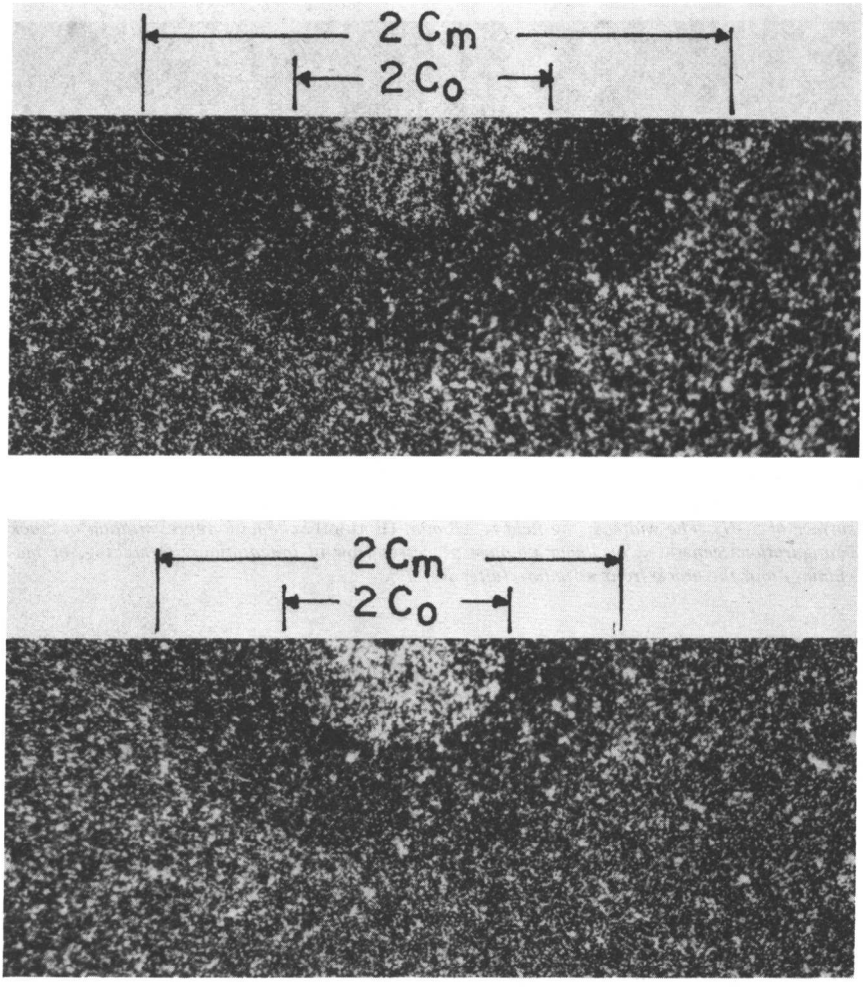

FIG. 5—*Fracture surfaces in Si_3N_4 (width of field 830 μm):* (Top) *Knoop indentation (50-N load) in a polished surface (specimen from Fig. 4*b*).* (Bottom) *Knoop indentation (50-N load) in a machined surface (after Ref* 17*).*

Machining Damage

Observations of Crack Response

With the acoustic scattering setup of Fig. 3, separate reflected signals were obtained from the cracks associated with the major grooves on machined surfaces of Si_3N_4 [*17*]. The variation of acoustic scattering from the strength-controlling crack during a failure test is shown in Fig. 7. The irreversible increase in scattered intensity indicates that a residual crack-opening stress